Mon. Not. R. Astron. Soc. **280,** 720–734 (1996)

The chemical composition of H II regions in the outer Galaxy

J. M. Vílchez[1,2] and C. Esteban[1,3]

[1]*Instituto de Astrofísica de Canarias, E-38200, La Laguna, Tenerife, Spain*
[2]*Department of Astronomy, University of Athens, Panepistimiopolis, 157 83 Zografos, Athens, Greece*
[3]*Instituto de Astronomía, UNAM, Ap. Postal 70-264, 04510 México D. F., Mexico*

Accepted 1995 November 29. Received 1995 November 27; in original form 1995 June 9

ABSTRACT

New spectroscopic observations, including the optical and near-infrared ranges, have been obtained for a sample of H II regions located towards the Galactic anticentre. The sample includes H II regions with known galactocentric distances, their ionizing stars having been clearly identified from previous work. The spectra correspond to low-to-intermediate excitation nebulae, ionized by one/few late O/early B star(s). The global parameters of the regions, as well as their physical parameters such as electron density and temperature, are presented. Abundances have been computed using direct (spectroscopic) determinations of the electron temperature for some of the objects or alternatively assuming an adopted electron temperature derived from photoionization model fitting. Overall, the data appear to show a substantially flat gradient for the nitrogen abundance, going up to 18 kpc of galactocentric distance, as well as a mild gradient, if any, for oxygen. The data points for sulphur, although less numerous, give abundances which are consistent with the behaviour observed for the other elements. The N/O ratio also presents a very flat gradient across the outer Galaxy, with a value similar to the one derived from observations of optical emission lines of H II regions in the solar neighbourhood.

Key words: ISM: abundances – H II regions – Galaxy: abundances – galaxies: abundances – galaxies: ISM – infrared: ISM: lines and bands.

1 INTRODUCTION

The chemical abundances in the interstellar medium (ISM) in gas-rich galaxies are observed to be different depending on the precise location within a given galaxy, and also from one galaxy to another. Since the nucleosynthesis of the different chemical elements occurs in stars of different masses, the study of the chemical abundances in the discs of spiral galaxies is a powerful method for understanding the history of star formation and evolution in these galaxies. These ISM abundances can be derived by making use of the spectra of ionized nebulae such as planetary nebulae (PNe) and/or H II regions. The existence of gradients of chemical composition in galaxies has been known since the pioneering work by Searle (1971). For the Milky Way (MW) the abundance gradient can be derived using PNe (e.g. Maciel 1992). When deriving the abundances representative of the current ISM values, the H II regions are preferred as a reference since the ionized gas in PNe may be affected by self enrichment produced by the central star. With respect to the abundances in H II regions, the work by Shaver et al. (1983) remains a most fundamental reference. Optical spectra were obtained for a sample of H II regions located between galactocentric distances of 5 and 12 kpc approximately, and, with the help of convenient radio observations, physical properties and abundances were derived. This work established the existence of a negative gradient of abundance of the elements heavier than helium in the disc of our Galaxy. Subsequent studies of the chemical evolution of the Galaxy have greatly benefited from this work (e.g. Tosi & Díaz 1985; Matteucci & Francois 1989; Ferrini et al. 1994).

None the less, the range of galactocentric distances spanning the regions studied by Shaver et al. (1983) is by itself limiting their work to the study of the H II regions within a range of galactocentric distance of some ± 4 kpc from the solar neighbourhood. Therefore, the sampling of the whole galactic disc was still poor, in particular towards the galactic anticentre region. This fact has also resulted in a handicap for the MW studies, compared with those for nearby external galaxies, thus limiting the application of models of

galaxy evolution. In particular, limiting those aspects of the models that describe the evolution of the outermost parts of the disc, i.e. the anticentre, which might be considered, at least from the point of view of the chemical evolution, to be much closer to the pre-galactic/early conditions in the MW.

Although distance determinations for the H II regions in the anticentre have always been very reduced in number and have large uncertainties, from the work of Fich & Blitz (1984) and Blitz, Fich & Stark (1982) new distances have been derived for a substantial set of H II regions in this zone. In addition, Chini & Wink (1984) performed a study of the outer rotation curve of the Galaxy combining photometry of ionizing stars with spectroscopy of H II regions; also, Hunter & Massey (1990; hereinafter HM90) derived the properties of the central stars of a set of outer H II regions and presented their distances. All of these studies are consistent with a value between 18 and 20 kpc of galactocentric distance for the effective edge of the star formation in the (optical) galactic disc (see also Moffat et al. 1979), but new evidence has appeared favouring massive star formation even beyond 20 kpc (De Geus et al. 1993).

Recently, Fich & Silkey (1991) (hereinafter FS91) have performed a spectroscopic study of a group of H II regions located towards the Galactic anticentre. They suggested the possibility of a rather flat N/H gradient extending to the outermost parts of the Galaxy. In FS91 only one H II region presents data including both [O II] λ3727 Å and [O III] $\lambda\lambda$4959, 5007 Å lines, and the quoted errors imply large uncertainties for the derivation of the abundance gradient. Nevertheless, FS91 favoured the existence of a rather flat N/H gradient in the outer Galaxy, and previous work on the outermost H II region S 266 (Manchado, Esteban & Vílchez 1989) seems to point in the same direction.

Recent work on abundances in external galaxies (e.g. Garnett & Shields 1987; Vílchez et al. 1988a; Torres-Peimbert, Peimbert & Fierro 1989; Díaz et al. 1991; Zaritsky, Kennicutt & Huchra 1994) has demonstrated the importance of complete sampling of H II regions in the discs in gaining a full understanding of the results in terms of the star formation history of the galaxies. A global fit to the whole radial abundance gradient may be (dangerously) biased by the relative absence of observational points in the outermost – and/or innnermost – galactic regions. Therefore, the study of the abundances of the distant anticentre H II regions is of great interest.

The determination of the abundances of the H II regions in the galactic anticentre from optical emission lines is a difficult task, mainly for the following reasons: (i) the low number of catalogued H II regions; (ii) H II regions are frequently faint and show extended diffuse structures; (iii) the regions suffer from a large foreground column density of material, which produces both a high reddening and a likely background contamination in non-spatially resolved spectra; and (iv) known distances to the H II regions in the anticentre, as already commented, are not very numerous and often less certain. In order to overcome these problems, we have obtained long-slit spectra using an efficient spectrograph–telescope combination, with a high signal-to-noise (S/N) ratio to allow good background subtraction. In addition, our observations cover a large range in wavelength, from the UV up to the near-infrared edge, allowing us to define better model constraints in those cases where the faintness of the nebulae precludes direct electron temperature determination. At the same time, all of the H II regions in the sample studied have been selected among those having information about their ionizing stars (identification, total number and spectral types) as well as from radio observations, including rms densities and temperatures.

Taking all of the above into account, fundamental physical parameters of the H II regions such as the ionization parameter, the total number of Lyman continuum photons and the effective temperature of the (main) ionizing star, are derived. These parameters have later been combined with the spectral information – which includes values of the electron density and temperature, as well as of the chemical abundances – and a suitable grid of photoionization models, in order to find a physical fit to the observations. That procedure we believe will produce an appropriate determination of the abundances and the nebular parameters. In the following section we present the observations and the data reduction. In Section 3 the results of the study are described, Section 4 is devoted to their discussion, and finally our main conclusions are summarized in Section 5.

2 OBSERVATIONS AND DATA REDUCTION

The observations were carried out in October 1991 and September 1992 at the Observatorio del Roque de los Muchachos (ORM), La Palma, using the 4.2-m William Herschel Telescope (WHT) with the ISIS double-arm spectrograph at the Cassegrain focus. The journal of observations is presented in Table 1. The slit centre and position angle were chosen according to the morphology and surface brightness of the nebulae as shown in the POSS plates and/or from recent work in the literature (Mampaso 1991; Hunter 1992, hereinafter H92). An EEV detector with 22.5-μm pixels was used for each arm. Typical seeing values were about 1 to 1.5 arcsec, and the slit width was set to 1.5 arcsec, having a total length of some 3 arcmin in the spatial direction. A dichroic was set at an effective wavelength of λ5400 Å in order to separate the spectral ranges of blue and red arms. Two gratings, 316R and 300B, giving 316 and 300 line mm^{-1} for the red and blue arms respectively, were used, with corresponding reciprocal dispersions of 60.4 and 62.2 Å mm^{-1} respectively. The final spectral ranges used are $\lambda\lambda$3590–5250 Å in the blue and $\lambda\lambda$5640–7340 Å and $\lambda\lambda$8300–10 000 Å in the red, with a similar effective spectral resolution of 4 Å FWHM. This set up allowed us to cover a wide spectral range from [O II] $\lambda\lambda$3727 Å in the blue up to the [S III] λ9532 Å and P8 λ9546 Å lines in the near-infrared. A total of eight anticentre H II regions were observed for this project: S 98, S 127, S 128, S 209, S 219, S 266, S 283 and BFS 31. The observations of the H II region S 298 have been already published in our previous work (Esteban et al. 1990) on spatially resolved spectroscopy of nebulae associated with Wolf–Rayet (WR) stars. S 298 corresponds to NGC 2359, which is associated with the WR nebula RCW 5. This nebula was also included in Shaver et al. (1983) and here we will use average physical properties and abundances corresponding to the main H II region, outside of the WR bubble.

Table 1. Journal of the observations. The quoted positions correspond to the slit centre.

Nebula	α (1950.0) (hh mm ss)	δ (1950.0) (° ' ")	P.A. (°)	Grating	$\Delta\lambda$ (Å)	Exposure (s)
S 98	19 57 10.1	+31 13 33	0	300B	3590–5250	2200
				316R	5640–7340	1000
				316R	8300–10000	1000
S 127	21 27 04.6	+54 23 41	180	300B	3590–5250	2500
				316R	5640–7340	1200
				316R	8300–10000	1200
S 128	21 30 37.1	+55 39 22	90	300B	3590–5250	2000
				316R	5640–7340	900
				316R	8300–10000	900
S 209	04 07 19.6	+51 02 02	350	300B	3590–5250	2600
				316R	5640–7340	1200
				316R	8300–10000	1200
S 219	04 52 28.1	+47 19 06	350	300B	3590–5250	2000
				316R	5640–7340	900
				316R	8300–10000	900
S 266	06 15 54.1	+15 18 08	0	300B	3590–5250	1200
				316R	5640–7340	500
				316R	8300–10000	600
S 283	06 35 53.9	+00 47 10	0	300B	3590–5250	2200
				316R	5640–7340	1000
				316R	8300–10000	1000
BFS 31	03 21 04.3	+54 46 22	350	300B	3590–5250	2600
				316R	5640–7340	1200
				316R	8300–10000	1200

The data reduction was performed at the IAC using the standard software package FIGARO (Shortridge 1990), following the standard procedure of bias subtraction, flat-fielding, wavelength calibration, sky subtraction and flux calibration. The correction for atmospheric extinction was performed using an average curve for the continuous atmospheric extinction at the ORM observatory (King 1985) and flux calibration standards from Oke (1974) and Stone (1977) were used throughout the observations.

The observations in the spectroscopic near-infrared range typically suffered from heavy atmospheric absorption, and therefore the calibration in this wavelength range is expected to present large uncertainties (e.g. Vílchez et al. 1988a; Díaz et al. 1991). None the less, the relatively high spectral dispersion used in the present study somehow alleviated the problem of unsaturated atmospheric absorption. However, as will be indicated later, the [S III] λ9532 Å line fluxes are normally strongly affected by absorption and, therefore, the measurements of the [S III] λ9069 Å line have been used in the derivation of the S^{++}/H^{+} abundances for all the regions, the only exception being S 266 for which measurements of both of the [S III] lines have been used.

3 RESULTS

3.1 Line intensities

Although for some objects in the sample a spatial study might have been performed, the high S/N ratio required make this task fairly difficult to perform for the whole sample, and therefore one-dimensional, high S/N ratio spectra were produced for each H II region integrating the total observed flux within the slit. An exception to this rule was the region S 266. The spectra of this region were of very good quality; they showed that the inner parts appeared to be dominated by the effects of a powerful stellar wind from the central star. Therefore, in this case we selected two zones in order to integrate the one-dimensional spectra, one corresponding to the central zone of the nebula (zone A) and the other to the external H II region (zone B). Fig. 1 shows the spectra of a representative H II region of the sample.

Line intensities were measured by integrating all of the flux in the line between two given limits and over a fitted local continuum. The measurements were performed with the help of the DIPSO software package (Howarth & Murray 1990). The spectra were corrected for reddening using the value of C(Hβ) derived from the observed quotients Hα/

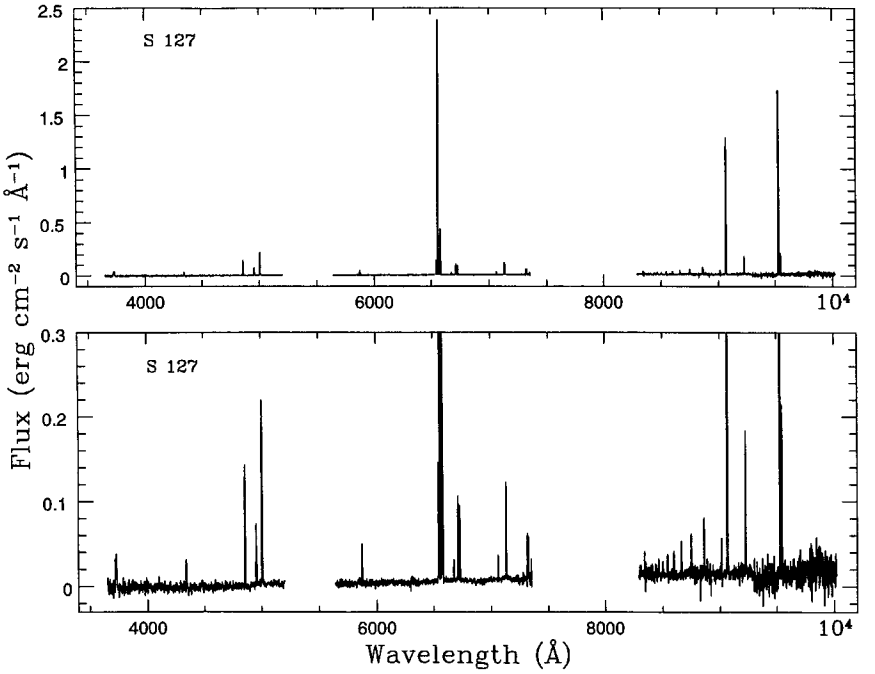

Figure 1. Representative observed spectra, including the three wavelength ranges, for the H II region S 127 (top); the same plot scaled down to Hγ (bottom). Flux scale is relative.

Hβ, Hγ/Hβ, Hδ/Hβ and taking into account the intensity ratio of the infrared Paschen lines to Hβ – when they have a high enough S/N ratio – as compared with the theoretical values expected for case B recombination using Brocklehurst (1971). The typical error in the reddening coefficients is estimated to be of the order of ± 0.15. The comparison with previous estimates of C(Hβ) by FS91 and H92 for some of the regions in common with this work gives general consistency, except in the case of S 127 for which we derived a value larger than the one quoted in FS91, whereas the region S 266 presented the opposite situation. The values derived for the reddening constant were large, as expected for this zone of the anticentre of the galaxy. This fact implies that there is a difficulty in detecting faint lines in the blue part of the spectrum, and also makes the reddening correction for the [O II]/Hβ and the [N II]/[O II] line ratios very important [e.g. for C(Hβ) = 2 the reddening correction for [O II]/Hβ is close to a factor of 3]. Line intensities that have been reddening corrected using the results of Whitford (1958) and normalized to Hβ = 100 are presented in Table 2. The quoted observational errors of the line intensities have been computed taking into account the uncertainties in the measurement of the lines and in the reddening coefficient.

3.2 Physical conditions and chemical abundances

Electron densities were derived for all of the observed regions using the [S II] $\lambda\lambda$6717/6731 Å ratio following the standard procedure (McCall 1984). Density values were in the low-density limit (≤ 100 cm^{-3}) for S 98 and S 285. In the rest of the cases the density values appear to be typically of several hundreds of particles per cm^3, with the highest measured values being 550 and 370 cm^{-3} for S 209 and S 127 respectively. The density values are consistent with previous determinations for the regions in common with FS91 and H92, although within a large dispersion, which can somehow be expected given the extended nature of the objects and the (likely) different slit placements. In some cases these differences were very high, as can be seen when comparing the value of 3500 cm^{-3} given by H92 for the electron density of S 219 with our more modest value of 90 cm^{-3} in the low-density limit.

Electron temperatures can be derived directly from the spectra of some of the observed regions. (As customary, all the values of the electron temperature throughout the paper are expressed in units of 10^4 K.) For S 127 and S 128, the value of t([O II]), the characteristic electron temperature in the O^+ zone, can be calculated from the ratio of the [O II] doublets $\lambda\lambda$7320, 7330/3727 Å. This is also the case for S 266, for which this line ratio can be determined from the spectra of both zones of the nebula. For this nebula, a value of the t([N II]) electron temperature – for the same ionization zone – can be derived using the [N II] $\lambda\lambda$5755/6584 Å line ratio. For S 298, the value of t([O III]), the electron temperature of the O^{++} zone, has been taken from Esteban et al. (1990). In the case of S 209, the uncertainty in the measurement of the [O II] λ3727 Å line flux precludes the derivation of a precise value of t([O II]), and only an upper limit was considered. Similarly, for S 219, owing to the uncertainty in the $\lambda\lambda$7320, 7330 Å line fluxes, the value quoted for t([O II]) is not useful, and therefore we did not consider the spectrum of S 219 for a direct determination of the abundances. Ionic and total abundances were computed for S 127, S 128 and S 266 using the derived electron temperature and density following the standard procedure (e.g. Pagel et al. 1992). As pointed out in Section 2, the flux in the [S III] λ9532 Å line was not used in the derivation of the

Table 2. Reddening corrected line intensities (Whitford 1958) normalized to Hβ=100. The dereddened Hβ flux $F(H\beta)$ in erg cm^{-2} s^{-1}, and the reddening coefficient $C(H\beta)$ are also presented.

Line	f(λ)	BFS31	S209	S219	S283	S98	S127	S128	S266 A	S266 B
3727 [OII]	0.26	63:	120:	275±27	400±45	372±81	252±31	211±25	76±13	225±28
3889 H8	0.22	–	–	–	–	–	–	–	9:	–
3969 H7	0.21	–	–	–	–	–	–	–	11:	–
4101 Hδ	0.18	–	–	29±10	34:	–	25±7	28±6	20±5	29±9
4340 Hγ	0.135	–	–	49±7	42±8	–	46±5	48±5	43±5	48±8
4861 Hβ	0.00	100±8	100±8	100±2	100±5	100±11	100±3	100±3	100±3	100±5
4959 [OIII]	−0.02	–	95±7	–	–	–	40±2	97±2	–	–
5007 [OIII]	−0.03	–	309±7	5:	35±4	41±14	127±10	291±4	≤1	≤1
5015 HeI	−0.03	–	–	–	–	–	–	–	3:	–
5200 [NI]	−0.07	–	–	–	–	–	–	–	4±1	14±5
5755 [NII]	−0.21	–	–	–	–	–	–	–	0.8:	2.3:
5876 HeI	−0.23	–	11±2	–	–	–	9±1	9±1	2.1±0.7	1.5:
6300 [OI]	−0.30	–	–	–	4±1	–	–	–	2.1±0.5	7±1
6363 [OI]	−0.31	–	–	–	–	–	–	–	0.8±0.3	1.8±0.6
6548 [NII]	−0.34	22±4	9±2	30±1	17±2	11:	14±2	13±3	9±1	38±5
6563 Hα	−0.34	286±33	268±30	286±31	286±31	286±32	250±25	269±31	273±30	316±35
6584 [NII]	−0.34	60±7	31±4	81±9	67±7	107±12	45±5	35±5	29±4	110±12
6678 HeI	−0.35	–	3±1	–	–	–	2.4±0.4	3.9±0.7	0.6±0.2	–
6717 [SII]	−0.36	39±5	7.7±1.1	39±5	44±5	30±4	9.1±0.8	10.9±1.4	12.1±1.5	53±5
6731 [SII]	−0.36	31±4	7.2±1.1	28±4	34±5	19±3	8.1±0.9	8.2±1.1	10.6±1.4	49±5
7065 HeI	−0.40	–	3.5±0.7	–	–	–	1.8±0.3	2.4±0.4	0.9:	–
7136 [ArIII]	−0.41	–	11.4±1.5	–	–	–	8±1	11±2	–	–
7320 [OII]	−0.43	–	2.3±0.4	3:	–	–	3.5±0.5	2.6±0.5	0.9±0.3	2.5±0.7
7330 [OII]	−0.43	–	2.9±0.5	–	–	–	3.1±0.5	2.2±0.5	0.6±0.2	2.5±0.7
8446 OI	−0.56	5.0±1.6	–	–	–	–	–	–	9±2	4±1
8467 P17	−0.56	–	–	–	–	–	0.8:	0.6±0.2	0.6±0.2	–
8502 P16	−0.56	–	–	–	–	–	0.6:	0.6±0.2	1.8±0.4	–
8545 P15	−0.57	–	0.3±0.1	–	–	–	0.7±0.1	0.8±0.2	1.9±0.4	–
8598 P14	−0.57	–	0.6±0.2	–	–	–	0.9±0.1	0.9±0.2	1.0±0.4	–
8665 P13	−0.58	–	0.8±0.3	1.2:	–	–	1.1±0.2	1.1±0.2	2.6±0.6	–
8750 P12	−0.59	–	0.7±0.2	–	–	–	1.3±0.2	1.2±0.2	1.4±0.3	1.5:
8862 P11	−0.60	–	1.0±0.3	–	–	–	1.7±0.3	1.8±0.3	1.8±0.4	2.5:
9013 P10	−0.62	–	1.2±0.2	1.3:	–	–	1.2±0.2	1.2±0.2	1.8±0.4	2.4:
9069 [SIII]	−0.64	2.3±1.0	19±4	11±2	7±2	11±3	26±5	30±6	0.4:	2:
9229 P9	−0.64	3:	2.7±0.5	2.5±0.7	–	5±1	3.0±0.5	3.4±0.7	2.3±0.5	4±1
9532 [SIII]	−0.65	–	11±2	4±1	23±5	22±5	33±5	33±7	1.8±0.5	9±2
9546 P8	−0.65	–	0.9:	–	–	–	4.0±0.6	3.1±0.6	3±1	3±1
F(Hβ) (10^{-13})		2.74	37.20	6.11	1.30	25.49	12.61	37.83	19.60	0.95
C(Hβ)		1.83	3.08	1.12	1.44	2.35	2.37	2.25	1.86	1.42

S^{++}/H^{+} ionic abundance for S 127 and S 128. A theoretical ratio [S III] λ9532 Å/[S III] λ9069 Å = 2.5 was assumed.

Chemical abundances and physical properties for the H II regions S 127, S 128 and for zone A and B of S 266, are presented in Table 3. The abundances and physical parameters for the rest of the regions are discussed in the following section.

4 DISCUSSION

4.1 Physical parameters and spectroscopic properties of the H II regions

The fundamental physical parameters of the H II regions are presented in Table 4, where we have included data for a more extended sample including some regions taken from FS91 with well-known ionizing stars. Columns 1 and 2 include the name and the galactocentric distance of the H II region. Distances have been taken from FS91 who compiled data from Moffat et al. (1979) and/or Blitz et al. (1982). The uncertainties are large in some cases and, on average, a factor of 20 per cent can be assumed as a safe limit to the relative error. In any case, the largest error in the distances quoted by FS91 occurs for S 266, with an error of 4.7 kpc for a galactocentric distance of 17.9 kpc. In column 3, the spectral type(s) of the ionizing star(s) is(are) quoted. Column 4 includes the value of the effective temperature of the central ionizing star according to Panagia (1973). In the case of several ionizing stars, the quoted value refers to the hottest spectral type. An estimation of the effective temperature based on the hardening of the ionizing spectrum (Vílchez & Pagel 1988) is included in parenthesis. The number of Lyman continuum ionizing photons, NLy_C, derived from the spectral type content (using Panagia 1973) is presented in column 5, as well as the value of the same parameter as derived from the total radio continuum flux in FS91 (following Lequeux 1980; HM90), which is included in parenthesis. The density of the nebulae measured from the [S II] ratio is shown in column 6, and column 7 includes the estimated value of the filling factor derived as $f=(N_{rms}/N_e)^2$,

Table 3. Chemical abundances and physical properties for the H II regions S 127 and S 128 and the two zones of S 266.

	S127	S128	S266 - A	S266 - B
t([OII])	$1.07^{+0.11}_{-0.08}$	$1.16^{+0.19}_{-0.16}$	$0.99^{+0.29}_{-0.16}$	$1.02^{+0.23}_{-0.14}$
t([NII])	–	–	1.30:	1.13:
12+log O^+/H^+	7.88±0.28	7.64±0.30	$7.47^{+0.43}_{-0.52}$	$7.90^{+0.34}_{-0.41}$
12+log O^{++}/H^+	7.58±0.22	7.82±0.20	≤5.59	≤5.54
12+log O/H	8.06±0.20	8.04±0.20	$7.48^{+0.43}_{-0.52}$	$7.90^{+0.34}_{-0.41}$
log N^+/O^+	$-1.02^{+0.25}_{-0.52}$	$-0.96^{+0.26}_{-0.56}$	$-0.72^{+0.32}_{-0.62}$	$-0.59^{+0.30}_{-0.58}$
12+log N/H	7.22±0.20	7.08±0.22	$6.74^{+0.27}_{-0.33}$	$7.31^{+0.22}_{-0.28}$
12+log S^+/H^+	5.52±0.18	5.49±0.18	$5.76^{+0.26}_{-0.32}$	$6.39^{+0.21}_{-0.26}$
12+log S^{++}/H^+	6.46±0.18	$6.47^{+0.14}_{-0.21}$	$4.97^{+0.27}_{-0.33}$	$5.66^{+0.21}_{-0.27}$
12+log S/H	6.51±0.18	$6.51^{+0.14}_{-0.21}$	$5.82^{+0.26}_{-0.32}$	$6.46^{+0.21}_{-0.26}$
log S/O	$-1.55^{+0.20}_{-0.50}$	$-1.53^{+0.16}_{-0.51}$	$-1.70^{+0.33}_{-0.70}$	$-1.44^{+0.28}_{-0.65}$
log Ar^{++}/O^{++}	$-1.77^{+0.22}_{-0.53}$	$-1.95^{+0.22}_{-0.56}$	–	–
10^2 $He^+/H^+(5876)$	6.7±0.9	9.2±1.1	1.5±0.7	1.1:
10^2 $He^+/H^+(6678)$	4.4±0.9	9.8±2.1	1.4±0.6	–
10^2 $He^+/H^+(7065)$	9.1±1.4	13.2±1.5	4.6:	–
10^2 $<He^+/H^+>$	6.9±1.0	10.2±1.7	1.7±0.8	1.1:
10^2 <He/H>	>5.6	10.7±1.7	>1.7	>1.1
log N_e([SII])	$2.57^{+0.28}_{-0.37}$	$2.04^{+0.61}_{-1.30}$	$2.51^{+0.37}_{-0.58}$	$2.62^{+0.26}_{-0.31}$

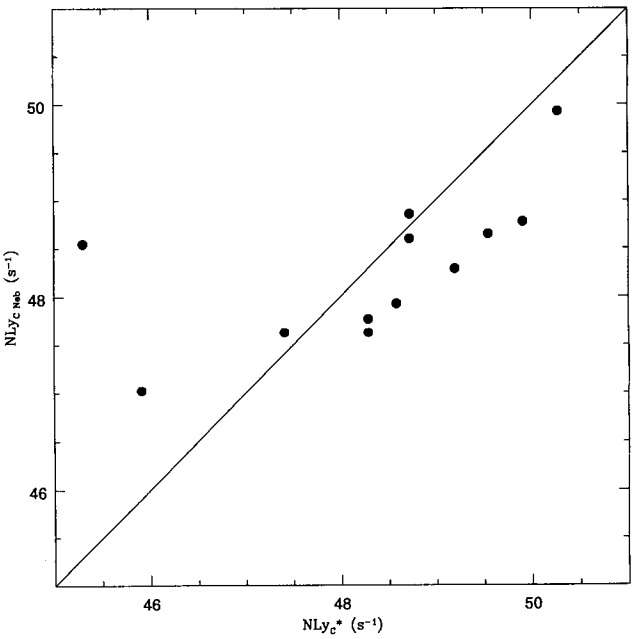

Figure 2. The total number of ionizing photons, summing for the spectral type(s) content, $N\mathrm{Ly}_{C*}$, versus the same quantity as derived from the total radio continuum flux, $N\mathrm{Ly}_{CNeb}$. Axes are in logarithmic scale. See the text for details.

Table 4. Fundamental physical parameters of the sample H II regions. R_{gc} (kpc) is taken from FS91, from which H II regions with known spectral type for their ionizing stars have been included in the sample. See the text for details.

REGION	Rgc	Sp. Type	$T^a_{eff}/10^3$K	LogNLy^b_C	N_e	$10^3 f$	LogU^b	Ref
S98	15:	O4V:	50.0:(35)	50.27 (49.93)	≤100			1, c
S127	15	O8V+2B0.5V	36.5 (35)	48.73 (48.60)	370	8	-3.86	1, d
S128	12.7	O7V	38.5 (36)	48.73 (48.86)	110	476	-2.85	1, d
S209	17	O9III+2B1III	33.0 (38)	49.91 (48.78)	548	0.3	-4.35	2
S211	14.1	O9V+B0V+O9I	34.5	49.20 (48.29)	250	37	-3.32	2,3
S212	14.2	O6I+B1III	38	49.55 (48.65)	≤100	≥34		2
S217	13.5	O8V+B2+2.5+3V	36.5	48.59 (47.93)				2
S219	12.5	B0V+B2.5V	30.9 (34:)	47.41 (47.63)	86	61	-3.91	3
S241	13.2	B1.5V	22:	45.30 (48.55)	≤100	≥7		3
S266	18	BeI?	— (30:)	— (47.89)	404	3	-4.40	4, e
S271	13.2	B0V	30.9	48.29 (47.77)				3
S283	17	B0V	30.9 (37:)	48.29 (47.63)	169	7	-4.15	5
S285	14.7	B1V	22.6	45.91 (47.02)	≤100	≥19		3
S298	13.6	WN5	67^f (50)	48.90^f (49.39)	≈100	≈12	≈-3.7	6, g
S301	12.9		40^h	— (49.05)	≤100	≥35		
BFS31	12.4		— (30:)		207			
BFS54	16.3		32^h	— (47.89)				
BFS64	11.7		34^h	— (48.12)	≤100	≥11	≥-4.16	

References. Spectral types after: (1) Mampaso (1991). (2) Chini & Wink (1984). (3) HM90. (4) Manchado et al. (1989). (5) Wouterloot et al. (1989). (6) van der Hucht et al. (1981).
Notes. (a) $T_{\rm eff}$ (10^3 K) of the hottest stellar spectral type, after Panagia (1973); in parentheses: $T_{\rm eff}$ (η) (10^3 K) after Vílchez & Pagel (1988). (b) Total $N\mathrm{Ly}_C$ photons for the sum of ionizing stars in column 3, using Panagia (1973); in parentheses: values of $N\mathrm{Ly}_C$ derived from radio continuum data (Fich & Silkey 1991) using Lequeux (1980) as in HM90. Log U is computed using the value of $N\mathrm{Ly}_C$ from the sum of ionizing stars. (c) Peculiar star. (d) Milky Way external arm? (e) Shell nebula. (f) Value taken from Esteban et al. (1993). (g) Wolf–Rayet ring nebula. (h) $T_{\rm eff}$ estimated from $N\mathrm{Ly}_C$, assuming only one equivalent main-sequence star from Panagia (1973).

N_{rms} being the rms density derived from radio observations taken from FS91. The value of the ionization parameter U is calculated directly from the quoted data from the expression $U \approx 2.7614 \times 10^{-20}$ $(N\mathrm{Ly_C}\ f^2\ N_e)^{1/3}$ (cgs). Notes and sources of the spectral classification of the central stars are included in the last column. As can be seen from the table, the H II region S 98 presents very discrepant values for the effective temperature and for the total number of ionizing photons, and the spectral type of the ionizing star is uncertain, suggesting a peculiar central ionizing star. In the cases of BFS 54, BFS 64 and S 301, the effective temperature is estimated from the total number of Lyman continuum photons, assuming only one ionizing star and ionization-bounded conditions. Overall, as shown in Fig. 2, there is good agreement between the number of ionizing photons estimated from the spectral type content, $N\mathrm{Ly_{C*}}$, and the one derived from the measurements of the radio continuum flux, $N\mathrm{Ly_{CNeb}}$. None the less, some regions seem to present lower values of the $N\mathrm{Ly_{CNeb}}$ for a given value of $N\mathrm{Ly_{C*}}$, which may be a signature of density-bounded conditions. In contrast, for two of the objects S 241 and S 285, there is a huge discrepancy between both values of $\log N\mathrm{Ly_C}$; in this case the value of $N\mathrm{Ly_{CNeb}}$ being bigger by a large factor. This last effect, if real, will be telling us that the actual total stellar content – and/or the true ionizing sources – of these nebulae is not well known.

In Table 5 we present the spectroscopic properties for the extended sample of H II regions. The table includes the values of the abundance parameter R_{23} (Pagel, Edmunds & Smith 1980), of the (equivalent) sulphur abundance parameter S_{23}, which can be defined as $S_{23} = ([\mathrm{S\,II}] + [\mathrm{S\,III}])/\mathrm{H}\beta$, and of the softening parameter, η' (Vílchez & Pagel 1988) which is a good indicator of the effective temperature. Also, the excitation measured by the [O III]/[O II] ratio, and the nitrogen-to-oxygen and nitrogen-to-sulphur line ratios [N II]/[O II], [N II]/[S II] respectively, are included in the table. Line ratios for the H II regions not observed here are derived from FS91. The last three columns of Table 5 show different values of the electron temperature: direct determinations from optical line ratios, $t([\mathrm{O\,II}])$, and/or from radio data (taken from FS91), t_{RL}, as well as the expected value from the empirical calibration, $\langle t_{R_{23}} \rangle$.

In Fig. 3 we show the ratios R_{23}, [N II]/[O II] and [N II]/[S II] versus galactocentric distance for the sample of H II regions. It can be seen that the values of [N II]/[O II] are quite homogeneous, clustering around $\log[\mathrm{N\,II}]/[\mathrm{O\,II}] \approx -0.7$, no matter the value of the galactocentric distance. A similar situation holds for R_{23}; for this parameter the values are around $\log R_{23} \approx 0.6$ and show no apparent correlation with galactocentric distance. In contrast, the ratio [N II]/[S II] shows an increase up to a galactocentric distance of about 16 kpc; beyond this galactocentric distance, however, the three outermost H II regions do not follow the same behaviour. On the other hand, for those cases where a value of the softening parameter η' can be derived, its anticorrelation with $N\mathrm{Ly_{CNeb}}$ is apparent, reflecting the expected trend between the effective temperature of main-sequence ionizing stars and the total number of ionizing photons.

A model-dependent electron temperature determination has been performed for all of the H II regions without a reliable direct measurement of t_e. This procedure is expected to produce an improved determination of the abundance when compared with the derivations of the abundance that make use of the standard empirical calibration. For each H II region, we have taken into account only those models that reproduce the spectroscopic parameters derived for the regions within the constraints found for the effective temperature of the ionizing star, the value of the ionization parameter and the filling factor – these parameters have been derived *ab initio* from direct measurements. We have selected all the low-density ($N_e \leq 100\ \mathrm{cm^{-2}}$) photoionization models from a grid (Stasińska 1980, 1982,

Table 5. Spectroscopic parameters for the sample H II regions. See the text for details.

REGION	$\mathrm{LogR_{23}}$	$\mathrm{Log}\eta'$	$\mathrm{LogS_{23}}$	O3/O2[a]	LogN2/O2[b]	LogN2/S2[c]	$t_{[OII]}$	t_{RL}	$\langle t_{R_{23}} \rangle$
S98	0.63	0.75	-0.05	0.11	-0.54	0.34			1.0
S127	0.62	0.90	0.03	0.50	-0.75	0.69	1.07	0.88:	0.8
S128	0.77	0.50	0.15	1.45	-0.74	0.25	1.16		0.9
S209	0.72	0.14	-0.30	2.71:	-0.54	0.32	≤1.4	0.88:	0.9
S211						0.42		0.38::	
S212	0.76			0.17	-0.85	0.27		0.67:	0.9
S217						0.20			
S219	0.45	1.50	-0.09	0.02:	-0.64	0.08	0.80:		0.9
S241	≥0.44				-0.50	0.03			≥0.6
S266	0.39		0.00	≤0.03	-0.39	0.03	1.02		
S271						0.26			
S283	0.65	0.32	0.14:	0.09	-0.77	-0.06			1.0
S285						-0.01			
S298	1.20	-0.30		4.00	-0.92	-0.08	1.40[d]	1.19:	
S301	≥0.14					0.20		0.77	≥0.6
BFS31	-0.20		-0.11:	≤0.03	-0.02	-0.07			0.5:
BFS64						-0.16			

Notes. (a) O3/O2 = [O III]5007/[O II]3727; (b) N2/O2 = [N II]6584/[O II]3727; (c) N2/S2 = [N II]6584/[S II]6717, 31; (d) $t_{[\mathrm{O\,III}]}$.

hereafter S80, S82) that have $T_{\rm eff}$, R_{23} and U consistent with the parameters presented in Tables 4 and 5. Subsequently, for each region the final adopted value of t_e has been interpolated from among those models that give a better fit to the observed spectroscopic ratios. In other words, the knowledge of $T_{\rm eff}$ and U, together with the value of the R_{23} parameter for each object, allows a solution to be found easily using the model grid as an interpolation device. In fact, a bivaluate solution is found in many cases, reflecting the bivaluate character of R_{23} with the O/H abundance. This uncertainty has been traditionally avoided using the [N II]/Hα ratio. This, however, may be a dangerous practice in

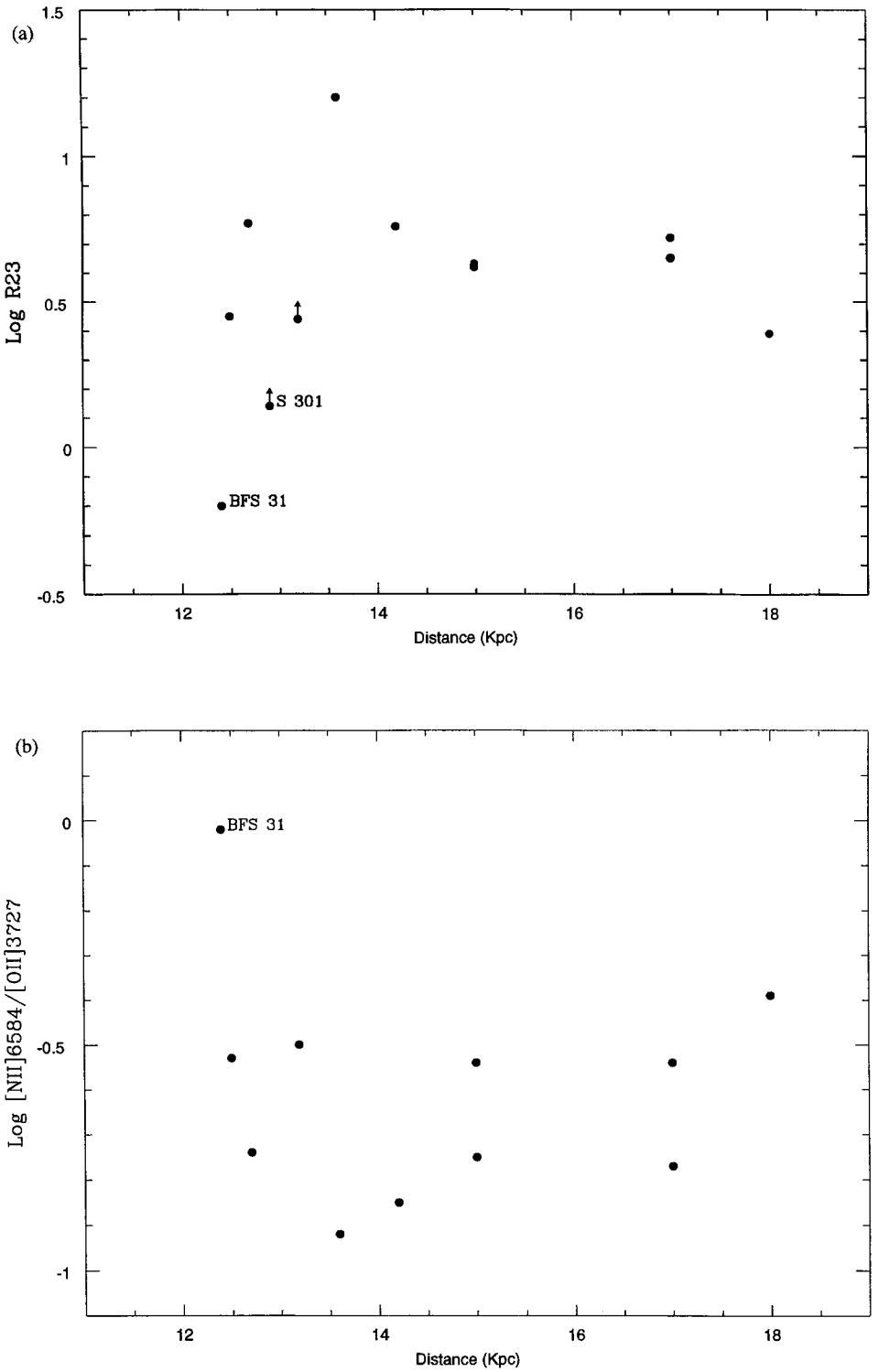

Figure 3. The ratios (a) R_{23}, (b) [N II]/[O II] and (c) [N II]/[S II] are shown versus the galactocentric distance for the whole sample of H II regions.

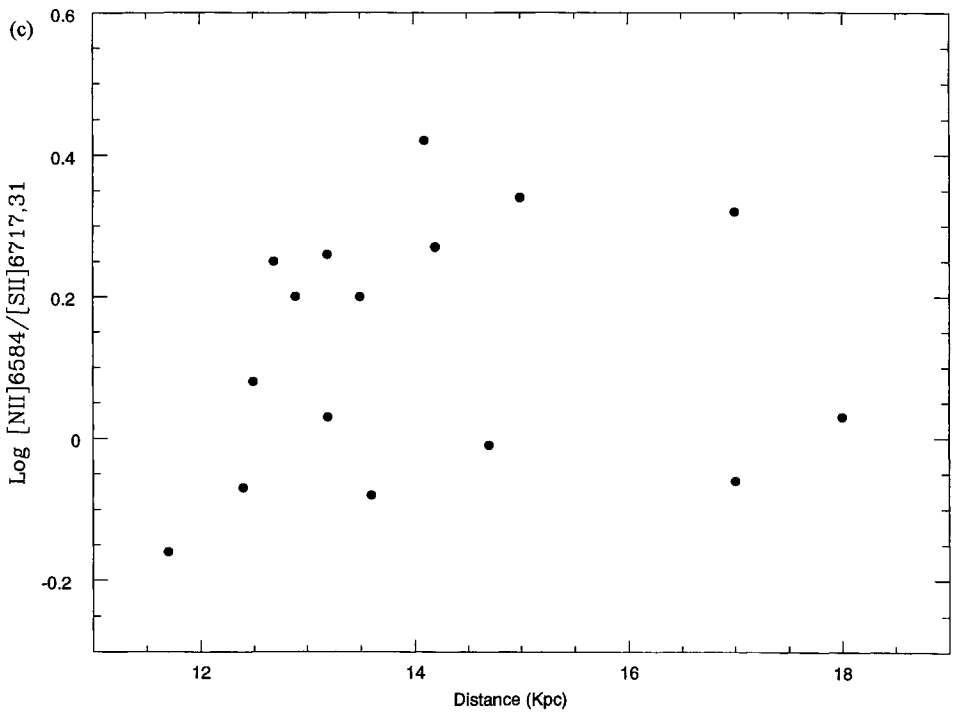

Figure 3 – *continued*

Table 6. Abundances for H II regions without direct electron temperature determination. The adopted electron temperature; the computed oxygen abundance O/H; the N^+/O^+ and N^+/S^+ ionic ratios; the nitrogen abundance N/H; the ionic and total sulphur abundances S^+/H^+, S^{++}/H^+ and S/H respectively; and the He^+/H^+ and total He/H abundances are included.

REGION	S98	S209	S211	S212	S217	S219	S241	S271	S283	S285	S298	S301	BFS31	BFS54	BFS64
$<t_{[OIII]}>_{Adopted}$	1.0	0.9	1.0	0.9	0.9	0.9	0.9	1.0	1.0	1.0	1.4	1.0	0.5	1.0	1.0
$<t_{[OII]}>_{Adopted}$						0.8									
12+Log O/H	8.2	8.3		8.5		8.5	8.4		8.2		8.2	8.4	8.4:		
Log N^+/O^+	-1.1	-0.9		-1.2		-1.1	-1.1		-1.1		-1.0		-0.6		
Log N^+/S^+	1.3	1.2	1.3	1.2	1.1	1.0	0.9	1.2	0.9	0.9	0.8	1.1	0.8		0.8
12+Log N/H	7.1	7.4	$\geq$7.3	7.4	$\geq$7.3	7.4	7.3	$\geq$7.3	7.1	$\geq$7.2	7.2	$\geq$7.0	7.8	$\geq$7.2	$\geq$7.1
12+Log S^+/H^+	6.0	5.7	6.0	6.0	6.2	6.4	6.4	6.1	6.2	6.3	5.8	5.9	7.2		6.3
12+Log $S^{++}/H+$	6.1	6.5				6.1			6.0		6.4		6.2		
12+Log S/H	6.4	6.6				6.6			6.4		6.5:		7.2		
10^2 He^+/H^+		8.4		8.8							10.0	8.2			
ICF		1.1:		1.1							1	1:			
10^2 He/H		9.2		9.7							10	8.2			

some cases. First, because it needs to assume a given behaviour for the N/O abundance ratio; and secondly, because the relative intensity of the [N II] lines compared with Hα may change within the region purely because of local excitation effects (this last warning applies also to the [O III]/Hβ ratio when used as the only oxygen abundance indicator).

For those H II regions for which we have derived a value of the S_{23} parameter, we can solve the R_{23} ambiguity, since photoionization models predict that, in contrast to R_{23}, S_{23} appears to behave as a monotonically increasing function of the sulphur abundance. As an example, S80 low-density models with NLTE stellar atmospheres of $T_{\rm eff}(10^3\,{\rm K})$ between 35 and 37.5, and solar metallicity, give $\log R_{23}$ between 0.5 and 0.6 and $\log S_{23}$ between 0.1 and 0.2. For 0.1 solar abundance models, although the values of $\log R_{23}$ remain identical to the solar metallicity ones, $\log S_{23}$ is between -0.1 and -0.2.

We have tested the method, applying it also to the H II regions in the sample for which we have derived the abundances directly from the t_e determination. An oxygen abundance similar to that in the direct case has been found for S 127, and values that are consistent, within ± 0.2 dex, for S 127 and S 266.

Table 6 presents the abundances derived for the sample of H II regions with the model-dependent t_e determination. The table shows the adopted electron temperature; the computed oxygen abundance O/H; the N^+/O^+ and N^+/S^+ ionic ratios; the nitrogen abundance N/H; the ionic and total sulphur abundances S^+/H^+, S^{++}/H^+ and S/H, respectively; and the He^+/H^+ and the total He/H abundance derived applying an ionization correction factor (ICF) (Vílchez 1989) already used to derive helium abundances in H II galaxies (Pagel et al. 1992).

For some of the H II regions in Table 6 that have line fluxes taken from FS91, information is not available for the [O II], [O III] and [S III] lines. These regions are included in the table but no oxygen abundances have been derived for them, and only lower limits to the nitrogen and sulphur abundances can be quoted. For these H II regions, the lower limits to the total sulphur and nitrogen abundances come from the derived ionic abundances. The N^+/S^+ ionic abundance ratio is not sensitive to the electron temperature and, therefore, the exact value of the adopted t_e is not important in this case.

4.2 The chemical abundances of the outer Galaxy

In Fig. 4 the abundances of oxygen, nitrogen and sulphur are presented for the sample of H II regions versus their corresponding galactocentric distances. Within the range of distances between 12 and 18 kpc, the maximum variation in the oxygen abundance goes from $12+\log(O/H)\approx 8.5$ to 7.9. In fact, the oxygen abundance for most (80 per cent) of the observed regions remains within a band of $12+\log(O/H)=8.2$ to 8.4.

The N/H abundance has been estimated for a large number of regions, roughly within the same range of distances. All of the derived nitrogen abundances present values between $12+\log(N/H)=7.1$ and 7.4, with a single excursion to the high N/H value for BFS 31, for which the line fluxes have, in fact, large errors.

In the case of sulphur, the number of H II regions with a determination of the total S/H abundance is small. In this respect, BFS 31 presents an abundance that is extreme and uncertain; and the global dispersion shown by the derived S/H abundances is somewhat larger, ≈ 0.4 dex. This fact may be a consequence of larger observational errors, together with the small number of H II regions with measurements available for the infrared [S III] lines. An average value for the sulphur abundance in the outer Galaxy of $\langle 12+\log(S/H)\rangle \approx 6.6$ can be obtained from our data (excluding BFS 31).

In Table 7 we present the slopes of the abundance gradient – in dex kpc^{-1} – for oxygen, nitrogen and sulphur, computed from least-squares fitting of the available H II region abundances in the outer and inner parts of the Galaxy. Columns labelled A, B and C show the gradients derived from three different fits to the data for the outer Galaxy which are shown in Fig. 4. In column A, the gradients have been computed using only the abundances derived for the (three) H II regions with a direct determination of t_e: S 127, S 128 and S 266. The values quoted in column B have been obtained using the abundances derived from the model-dependent method for all the regions, while in column C we show the gradients derived including the abundances obtained from direct determination of t_e, together with those derived using the model-dependent procedure for the rest of the objects in the sample. In all cases the data for BFS 31 have been excluded from the fit owing to their large observational errors. A typical uncertainty for the computed gradients of ± 0.020 dex kpc^{-1} has been estimated assuming a conservative error for all the abundances used in the fit of ± 0.3 dex. Table 7 shows also the corresponding gradients obtained by Simpson et al. (1995) and Shaver et al. (1983) from data of H II regions in the inner Galaxy, scaled to $R_\odot = 8.5$ kpc. In the case of O/H the gradients computed in A, B and C are consistent, taking into account the estimated uncertainties, and appear somewhat flatter than the value obtained by Shaver et al. (1983). This can be seen in Fig. 4, where we have compared the O/H gradient obtained for the anticentre with the linear extrapolation of the Shaver et al. (1983) one.

In the case of nitrogen, the gradient obtained for the anticentre is clearly much flatter than the one obtained for the inner Galaxy. From the values of the slopes quoted in Table 7, and taking into account that the positive slope obtained in A is based on only three points, we can say that the N/H gradient in the anticentre turns out to be essentially flat, even considering the estimated uncertainties. Although we have not included N^+/H^+ lower limits in the computation of the gradient, the low-ionization conditions of the corresponding nebulae indicate that these values must be very close to the total N/H abundance. Bearing this in mind, the position of the lower limits in Fig. 4 gives additional support to the flattening of the outer gradient of nitrogen.

In the case of sulphur, our results also suggest some flattening of the gradient going towards the anticentre and, indeed, the values computed appear to be considerably lower than that obtained by Simpson et al. (1995) from IR fine-structure lines.

Of especial interest are the derived ionic ratios of N^+/O^+ and N^+/S^+. From photoionization models (e.g. S80; S82; Garnett 1990), we know that the N/O abundance ratio is equal to the N^+/O^+ ionic abundance ratio for objects with abundance lower than solar. Therefore, the N/O gradient can be delineated straightforwardly from our N^+/O^+ data. This is not straightforward, however, for the N^+/S^+ ionic ratio, for which a T_{eff}-dependent ICF is needed in order to derive N/S. Those regions with derived abundances of N/H and S/H in Table 5 that have a known T_{eff} have been used to derive an empirical ICF. Assuming that the ionic ratio is proportional to the N/S one, we derive an ICF $\approx 1/3$, which translates into the empirical relation $\log(N/S)\approx -0.5+\log(N^+/S^+)$. For S 266, the very low excitation of the nebula simplifies the use of N^+/S^+ as an abundance indicator; since neither N^{++} nor O^{++} is expected, and nearly all the sulphur is in the form of S^+, we expect $N^+/S^+ = N/S$. In doing so, we obtain $\log(N^+/S^+)=0.99$ and 0.92 fo S 266 A and B respectively. Furthermore, the total nitrogen abundance is then nearly equivalent to the ionic N^+/H^+ abundance.

Fig. 5 shows the behaviour of N/O and N^+/S^+ versus galactocentric distance for the observed regions. The derived values of N/O cluster around $\log(N/O)\approx -1.0$ no matter their galactocentric distances. The largest values derived for the N/O ratio are found in S 266 and BFS 31. Again BFS 31 present a value that has probably been over-

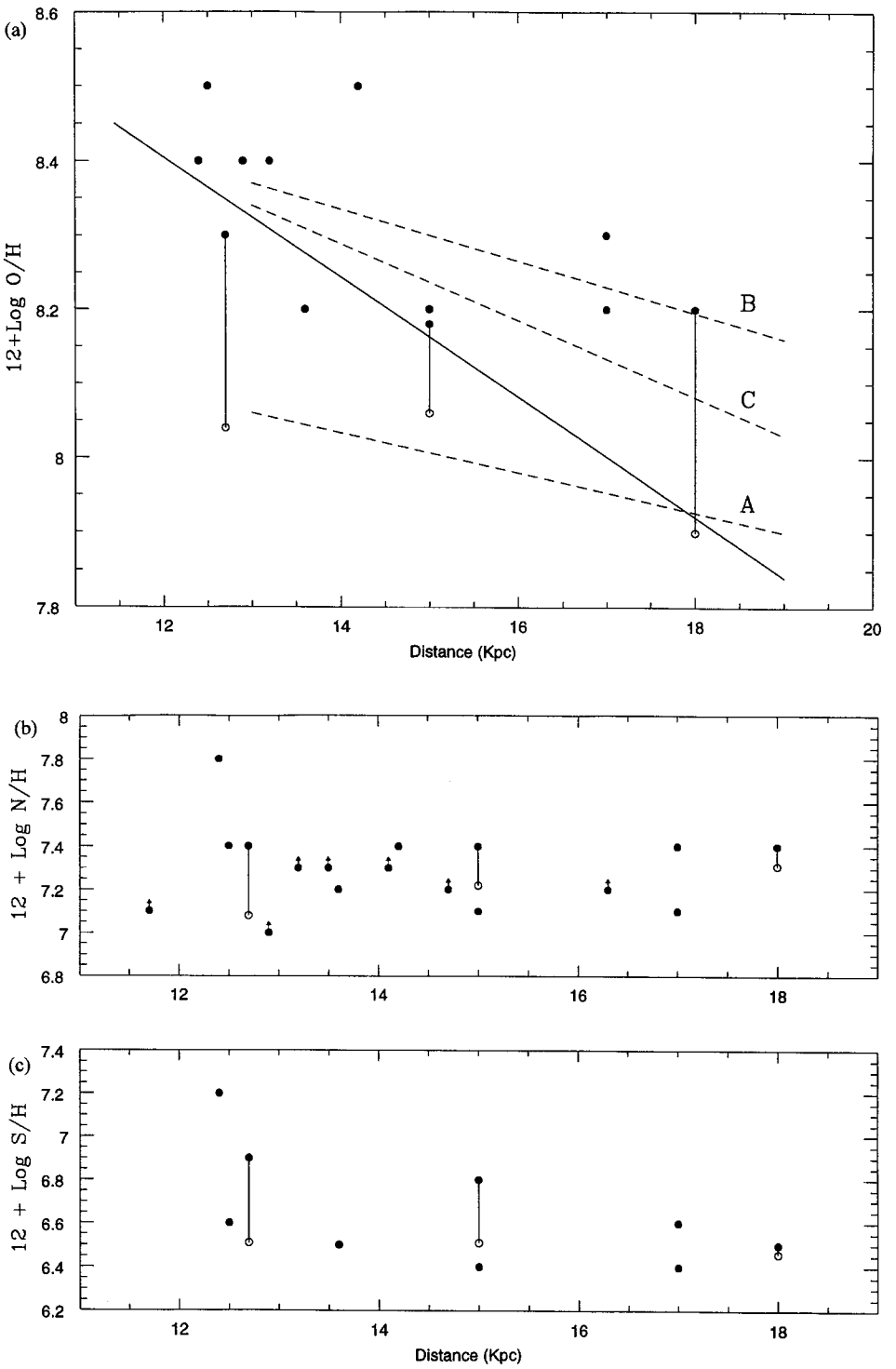

Figure 4. (a) The abundance of oxygen versus galactocentric distance for the anticentre H II regions. For S 127, S 128 and S 266 the abundances from direct t_e determination (empty circles) and from the model-dependent method (filled circles) are shown connected by a line. The A, B and C fits to the oxygen abundance gradient, as quoted in Table 7, are shown (dashed lines), as well as the extrapolation of the gradient derived by Shaver et al. (1983) (continuous line). (b) and (c) are the same for nitrogen and sulphur respectively. Lower limits to N/H abundances are indicated by an arrow.

estimated. The case of S 266 is most interesting. Given the peculiar nature of its (Be I?) central star, it may be expected that certain effects related to the presence of a strong stellar wind are in play. In particular, excitation by (localized) low-velocity shocks may influence the derivation of the physical conditions and, consequently, may alter our abundance analysis which has been performed assuming pure photoionization. The fluxes of the [N I] and [O I] lines for S 266

Table 7. The derived abundance gradients in the Galaxy (in dex kpc^{-1}).

	Outer Galaxy			Inner Galaxy	
	A	B	C	Shaver et al. (1983)	Simpson et al. (1995)
dlog(O/H)/dR$_G$	−0.028	−0.036	−0.051	−0.081	–
dlog(N/H)/dR$_G$	+0.043	−0.009	+0.002	−0.121	−0.100
dlog(S/H)/dR$_G$	−0.010	−0.041	−0.013	+0.005	−0.070

(A) Least-squares fit including only S 127, S 128 and S 266 (using abundances from direct determination of t_e).
(B) Least-squares fit including abundances derived from model-dependent methods for all the objects.
(C) The same as in B, but including abundances from direct determination of t_e for S127, S 128 and S 266.

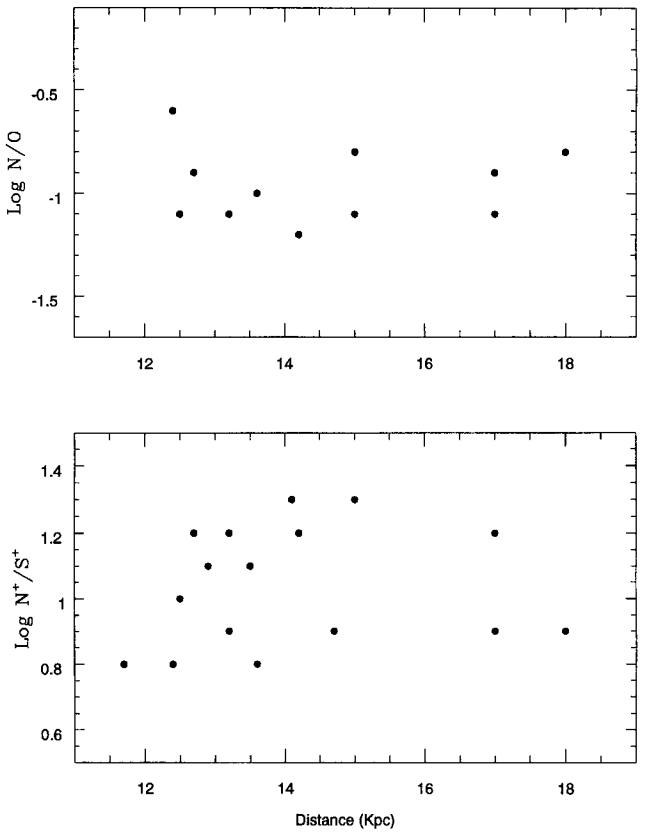

Figure 5. The behaviour of N/O (top) and N^+/S^+ (bottom) versus galactocentric distance for the observed H II regions.

quoted in Table 2 may be indicative of the coexistence of different excitation conditions. On the other hand, the possibility of local pollution by the wind of the central star of S 266 cannot be disregarded, and therefore the derived value of N/O must be adopted with some caution.

Only a few values have been derived for the total helium abundance, and these have high uncertainties. This is a direct consequence of the predominance of somewhat later spectral types for the ionizing stars, as shown in Table 4. In any case, the values derived for the helium abundance are consistent with the abundances expected from the observations in the solar neighbourhood.

Nitrogen is believed to be a secondary element, produced in the CNO burning of previously made carbon and (also) oxygen. This nitrogen production is returned into the ISM via PNe and the stellar winds of the more massive stars. For a truly secondary element, chemical evolution predicts that its yield must be proportional to the abundance of the primary progenitor(s). In the case of nitrogen and assuming the simple model of chemical evolution without infall, the N/H abundance should follow the O/H one as fast as $(O/H)^2$. The nitrogen yield will also depend on the exact trend of the carbon abundance, which may not necessarily follow that of oxygen in the Galaxy. Nevertheless, this last behaviour is not generally observed. On the other hand, a substantial scatter is present in the data, and whether it is physical or owing to error propagation seems still a matter of intepretation. However, the overall picture of the chemical composition of galaxies seems to indicate that there are two main regimes in the N/O versus O/H relationship. At low metallicities, $12+\log(O/H)\leq 8.3$, most of the galaxies appear to show an abundance ratio of around $\log(N/O)\approx -1.46$ (Garnett 1990). It has been claimed that this abundance level reflects the proportion of the true primary production of nitrogen; but still within this abundance range, some galaxies show N/O values that are extreme, well outside of the average behaviour. Outstanding cases are NGC 5253 and NGC 6822 (Garnett 1990; Pagel 1995). For higher abundances, H II regions in spiral galaxies show a global increase of the N/O ratio with O/H abundance. However, no universal proportionality relation is observed. The total variation in N/O appears different for each galaxy, the ratio being a reasonable amount higher for the early-type galaxy M 51 (Díaz et al. 1991), for example, than for the dwarfish, later type M 33 (Vílchez et al. 1988b). In our Galaxy the N/O points for the Sun, Orion and M 17 all favour values of $\log(N/O)\geq -0.9$, over a range of $\times 3$ in O/H. In the inner Galaxy, the N/O ratio has been derived using infrared lines of N^{++} and O^{++} (Rubin et al. 1988). These authors find much less evidence for a gradient in N/O across the Galaxy, although Simpson et al. (1995), from improved data, appear to find a rather steep gradient in the inner parts. It is worth mentioning here that infrared data give N/O values that are systematically higher than those derived from optical lines. We think the available information now argues against associating the nitrogen abundances in dwarf H II galaxies with those found in H II regions in

spirals. Our data show that the N/O ratios in the outer disc are not very different from the typical values derived for H II regions in the solar neighbourhood, and remain substantially unchanged up to the endpoint of the star formation in the disc, where we derive oxygen abundances close to $12+\log(\mathrm{O/H})=8.0$, typical of the H II regions in the Small Magellanic Cloud (SMC). In contrast, the average N/O ratio for the SMC is $\log(\mathrm{N/O})\approx -1.5$ (Garnett 1990). Our results for the N/O ratio appear to be consistent with the results of Dinerstein et al. (1993), obtained using far-infrared lines to study abundances for three H II regions in the anticentre (two in common with us: S 209 and S 212), who find an average value of $\log(\mathrm{N/O})=-0.90$. There has been some discussion in the literature over whether or not there is a gradient in S/O in external galaxies. From our data for the anticentre of the Galaxy we have found comparable slopes for the oxygen and sulphur gradients. Therefore, taking into account the limited data available for sulphur, we can say that there is no evidence favouring a substantial gradient in S/O in the anticentre.

In Fig. 6 we have shown the global gradients of O/H, N/H and S/H for the disc of the Galaxy, including observations from Shaver et al. (1983), FS91 and from this work. Shaver et al. (1983) points – shown corrected to $R_{gc}=8.5$ kpc – and FS91 data have been taken from the compilation of Mollá (1993). For the H II regions in common with these works the abundance points are shown connected by a line in the figure. An overall agreement is present among all the H II region data. The abundances derived from H II region spectra can be compared with the corresponding quantities derived from observations of B stars (Kaufer et al. 1994; Kilian-Montenbruck, Gehren & Nissen 1994, and references therein) for a common range of galactocentric distance. The stellar abundance gradients of oxygen and nitrogen derived by Kaufer et al. and by Kilian-Montenbruck et al., for the approximate range $7\leq R_{gc}\leq 15$ kpc, are virtually identical within 0.15 dex, well below the dispersion of their data. The stellar abundance gradient for sulphur has been derived by Kilian-Montenbruck et al. (1994). In Fig. 6, the stellar abundance gradients for O/H, N/H and S/H after Kilian-Montenbruck et al. (1994) are illustrated with a solid straight line. It is apparent that stellar and H II region oxygen abundances agree well for those regions close to the solar galactocentric distance, although the oxygen abundances of the innermost H II regions can be higher than the corresponding stellar points by some 0.5 dex. A similar situation holds for sulphur and nitrogen. For this last element, however, the N/H gradient derived from B stars at galactocentric distances beyond 9 kpc is found to give abundances systematically higher than the average value for H II regions (see Kaufer et al. 1994). This effect, if real, may be of great importance, but we need a larger number of observations before a firm conclusion can be reached. On the other hand, as already pointed out in Kaufer et al. (1994), any systematic offset between the abundances derived from H II regions and those coming from stellar data may be also caused by the use of different atomic data.

It therefore seems well established, from the comparison of stellar and H II region data, that a flatter abundance gradient is present in the outer part of the galactic disc, in contrast with the very steep one, as shown by the H II region data, that seems to be present for galactocentric distances

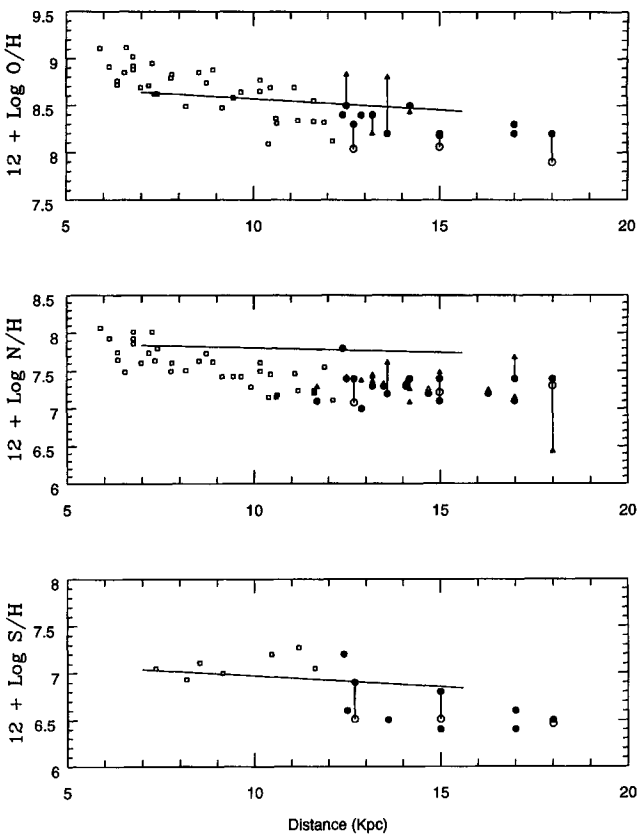

Figure 6. The global gradients of O/H, N/H and S/H in the Milky Way from 5 kpc onwards. Data from Shaver et al. (1983): empty squares; FS91: empty triangles; and for this work, filled and empty circles have been assembled. Abundance points corresponding to the same object are connected. The abundance gradients derived from B stars are illustrated by straight solid lines. The Shaver et al. (1983) points are taken scaled to a solar galactocentric distance of 8.5 kpc after Mollá (1993).

smaller than approximately 7 kpc. The combination of such a smooth oxygen gradient in the outer disc plus a steeper one in the inner Galaxy is apparent in Fig. 6. Such a shape may be also present in the nitrogen and sulphur gradients (e.g. Simpson et al. 1995). A radial change in the slope of the abundance gradient has been claimed for several nearby galaxies, and its relationship with some fundamental parameters of the galaxies, such as their effective radius or the presence/absence of a bar-like feature, has been already discussed, and it may be a common feature (e.g. Díaz 1989; Vila-Costas & Edmunds 1992; Edmunds & Roy 1993; Zaritsky et al. 1994). However, recent findings based on a reanalysis of the H II region abundance data in the literature for several well-known nearby spirals have pointed out the lack of any clear systematic behaviour in their abundance gradient slope (Henry & Howard 1995).

In principle, one may expect that closed-box models of chemical evolution using a simple parametrization of the observed gas-fraction profile (e.g. Pagel 1995) would predict that the logarithmic abundance gradient must become steeper when going outwards along the disc. To avoid this effect it is necessary to invoke the existence of inflow and possibly also radial gas flows driven by the inflow, as was

illustrated in the models of Major & Vigroux (1981). Their model with radial inflow gives gradients which are slightly steeper in the inner disc and somewhat shallower (in log units) in the outer parts. Very successful chemical evolution models of the Milky Way were later developed by Matteucci & Francois (1989). These models predict a change in the slope of the abundance gradient between some inner ($\Delta R_{gc}=4$–10 kpc) and outer ($\Delta R_{gc}=10$–14 kpc) portions of the disc, including infall of both primary and processed matter. Typical slopes for the inner and outer oxygen gradient in the primary infall model are $\Delta\log(O/H)/\Delta R=-0.11$ and -0.045 respectively (for $R_{gc\odot}=10$ kpc), values which turn out to be very close to the observations. On the other hand, many models assuming also gas infall and radial flows have been developed (see Edmunds & Greenhow 1995), some of them accounting for the (temporal) evolution of the abundance gradient in spiral galaxies (e.g. Köppen 1994). In this last work, abundance gradients may be steepened or flattened by inflow or by outflows, depending on the velocity field. However, perhaps as a consequence of the scarcity of abundance data, model predictions for the abundances of the outermost disc ($14\leq R_{gc}\leq 20$ kpc) are still missing. As discussed below, a simple extrapolation of the model gradients available towards extreme galactocentric distances now seems very risky and does not produce an appropriate fit to the observations.

The derived nitrogen abundance gradient may give us an extra clue to understanding the evolution of the outer Galaxy. Chemical evolution models such as those by Matteucci & Tosi (1985), including primary nitrogen production by intermediate-mass stars expelled by homogeneous winds, do not seem to produce values higher than $\log(N/O)\approx -1.0$ for oxygen abundances below $12+\log(O/H)\approx 0.8$. The derived nitrogen gradient appears flatter, as compared with the direct extrapolation beyond 14 kpc of the outermost slope delineated by current chemical evolution models (e.g. Matteucci & Francois 1989; Ferrini et al. 1994). In any case, these models have been developed to fit within the constraints observed for other areas of the galactic disc. The relatively high N/O abundance ratios derived for the H II regions in the outermost Galaxy are indicative of some previous substantial enrichment by intermediate mass stars. Recent chemical evolution models (Marconi, Matteucci & Tosi 1994) intended for the study of the abundances in blue compact galaxies (BCDs) can reproduce even higher N/O ratios for very low O/H abundances [$12+\log(O/H)\leq 8.0$], somehow supporting the dispersion observed for BCDs. These models include the various types of supernovae plus the effect of differential galactic winds powered by SNe II. These differential winds are such that only the fast, oxygen-rich SNe II material can actually leave the Galaxy. However, both the number of bursts and the wind efficiency should be changed from galaxy to galaxy in order to match with the observations. Therefore, every galaxy would follow its particular evolution on the N/O versus O/H diagram. After several (approximately seven) bursts of star formation, with Salpeter's initial mass function, followed by medium strength differential Galactic winds, these models can reach N/O abundance ratios similar to the ones observed in the outer Galaxy. However, invoking the existence of selective Galactic winds in order to understand the abundance data of the outer Galaxy, although may be somehow appealing, appears to us highly unrealistic, mainly because these winds must be forced to operate the same effect over all the vast region of the outer disc where the N/O ratio is found to be constant. This is, of course, a fairly different situation from what is believed to be happening in BCDs, where star-forming regions are localized bursts within a compact area of these shallower potential well galaxies.

Recalling the former hypothesis of Edmunds & Pagel (1978), the N/O ratio may be understood in the context of an 'evolutionary clock', assuming that the bulk of nitrogen is produced, as a primary element, in stars of intermediate mass (1 to 2.5 $M_\odot$). In such conditions the N/O ratio indicates the amount of time that has passed since the last most important burst of star formation, and therefore it may be considered as a measure of the age of the Galaxy. The lack of an obvious gradient in N/O, independent of the O/H measured for most of the observable disc – including the anticentre – may then be explained as a consequence of its high 'age'. Using the N/O ratio provides an extra bonus, since this will remain substantially unaffected under inflow and/or radial flows which, however, can modify the absolute values of element abundances. It follows that the chemical history of the ISM of both the inner and the outer disc has included a substantial contribution from intermediate-mass stars, and that these two dynamically distinct parts of the galaxy should have, roughly, a similar 'age'.

Although a higher past star formation rate in the outer Galaxy appears necessary to understand the observations, a subsequent decrease in the star formation activity would help to match it up with the present-day star formation rate derived for galactocentric distances of around 18 kpc and beyond in the galactic anticentre (De Geus et al. 1993). This change may have happened less than 1 Gyr ago, therefore allowing the nitrogen abundance to rise up to the observed value. A consequence of this picture for the history of star formation will be to impose some restrictions on inflow models, if one is to believe that *massive* gas inflows can be a good triggering mechanism for active star formation. Massive inflows have been invoked to trigger star formation since they appear to favour cloud–cloud collision, but the observations show that extended, active, star-forming complexes are not present in the Galactic anticentre.

5 CONCLUSIONS

We have performed optical and near-infrared spectroscopy for a sample of H II regions located in the Galactic anticentre. The observed spectra are characteristic of low-to-intermediate excitation nebulae, having typically one ionizing star with spectral type late O/early B. Global parameters of the H II regions, such as the ionization parameter, the number of Lyman continuum photons or the effective temperature of the ionizing star, have been derived as well as physical parameters such as the electron density and temperature.

We have derived O/H, N/H, S/H and He/H abundances for the sample using direct determination of the electron temperature for some H II regions or, alternatively, from photoionization model fitting. It has been found that the nitrogen abundance gradient, up to 18 kpc of galactocentric

distance, appears to be nearly flat, and a similar result appears to be consistent with the data for oxygen and sulphur.

A global analysis has been performed, including our abundances and a sample of data from the literature for H II regions at different galactocentric distances, taken from the works of Shaver et al. (1983) and Fich & Silkey (1991). It is apparent that the oxygen and nitrogen abundance gradients have two different parts, the slope of the inner gradient for $R_{gc} \leq 6$ kpc, being very steep while the gradient across the outer Galaxy remains nearly flat. Similarly, the comparison with published oxygen, nitrogen and sulphur abundance data obtained for B stars, with approximate galactocentric distances from 7 up to 15 kpc, gives consistent results for stellar and nebular abundances except, perhaps, in the case of nitrogen, for which the abundances derived from stellar spectra appear larger by some 0.4 dex. The derived N/O abundance ratio presents also nearly constant values along the observed portion of the disc, similar to the ones found for the H II regions in the solar neighbourhood.

Our work may favour a chemical history for the outer disc involving substantial contribution from intermediate-mass stars, plus a high (past) star formation rate more than 1 Gyr ago, which has now decreased to the estimated low present value.

ACKNOWLEDGMENTS

We thank Bernard Pagel and Manuel Peimbert for their stimulating suggestions on an earlier version of the paper and Don Garnett for his many helpful comments. Thanks are also given to Professor N. Voglis and the Department of Astronomy, University of Athens, for support and hospitality. This work has been partially financed by grants DGICYT No. PR94-199 for staff mobility, PB91-0531 and IAC P14/86.

REFERENCES

Blitz L., Fich M., Stark A. A., 1982, ApJS, 49, 183
Brocklehurst M., 1971, MNRAS, 153, 471
Castañeda H. O., Vílchez J. M., Copetti M. V. F., 1992, A&A, 260, 370
Chini R., Wink J. E., 1984, A&A, 139, L5
De Geus E. J., Vogel S., Digel S. W., Gruendl R. A., 1993, ApJ, 413, L97
Díaz A. I., 1989, in Beckman J., Pagel B. E. J., eds, Evolutionary Phenomena in Galaxies. Cambridge Univ. Press, Cambridge
Díaz A. I., Terlevich E., Vílchez J. M., Pagel B. E. J., Edmunds M. G., 1991, MNRAS, 253, 245
Dinerstein H. L., Haas M. R., Erickson E. F., Werner M. W., 1993, BAAS, 25, 850
Edmunds M. G., Greenhow M., 1995, MNRAS, 272, 241
Edmunds M. G., Pagel B. E. J., 1978, MNRAS, 185, 77P
Edmunds M. G., Roy J. R., 1993, MNRAS, 261, L17
Esteban C., Vílchez J. M., Manchado A., Edmunds M. G., 1990, A&A, 227, 515
Esteban C., Smith L. J., Vílchez J. M., Clegg R. E. S., 1993, A&A, 272, 299
Ferrini F., Mollá M., Pardi M. C., Díaz A. I., 1994, ApJ, 427, 745
Fich M., Blitz L., 1984, ApJ, 279, 125
Fich M., Silkey M., 1991, ApJ, 366, 107 (FS91)
Fich M., Blitz L., Stark A. A., 1989, ApJ, 342, 272
Garnett D. R., 1990, ApJ, 363, 142
Garnett D. R., Shields G. A., 1987, ApJ, 317, 82
Henry R. B. C., Howard J. W., 1995, ApJ, 438, 170
Howarth I. D., Murray J., 1990, SERC Starlink User Note No. 50, Rutherford Appleton Laboratory
Hunter D. A., 1992, ApJS, 79, 469 (H92)
Hunter D. A., Massey P., 1990, AJ, 99, 846 (HM90)
Kaufer A., Szeifert T. M., Krenzin R., Baschek B., Volf B., 1994, A&A, 289, 740
Kilian-Montenbruck J., Gehren T., Nissen P. E., 1994, A&A, 291, 757
King D. L., 1985, La Palma Technical Notes No. 15
Köppen J., 1994, A&A, 281, 26
Lequeux J., 1980, in Maeder A., Martinet L., eds, Star Formation. Geneva Observatory, Sauverny, p. 77
Maciel W. J., 1992, in Elements and the Cosmos. Cambridge Univ. Press, Cambridge, p. 210
Major D., Vigroux L., 1981, A&A, 98, 1
Mampaso A., 1991, PhD thesis, Universidad de La Laguna
Manchado A., Esteban C., Vílchez J. M., 1989, in Tenorio-Tagle G., Moles M., Melnick J., eds, IAU Colloq. 120, Structure and Dynamics of the Interstellar Medium. Springer-Verlag, Berlin, p. 120
Marconi G., Matteucci F., Tosi M., 1994, MNRAS, 270, 35
Matteucci F., Francois P., 1989, MNRAS, 239, 885
Matteucci F., Tosi M., 1985, MNRAS, 217, 391
McCall M. L., 1984, MNRAS, 208, 253
Moffat A. F. J., Fitzgerald M. P., Jackson P. D., 1979, A&AS, 38, 197
Mollá M., 1993, PhD thesis, Universidad Autonoma de Madrid
Oke J. B., 1974, ApJS, 27, 21
Pagel B. E. J., 1995, in Muñoz-Tuñon C., ed., VIAC Winter School Galaxy Formation and Evolution. Cambridge Univ. Press, Cambridge, in press
Pagel B. E. J., Edmunds M. G., Fosbury R. A. E., Webster B. L., 1978, MNRAS, 184, 569
Pagel B. E. J., Edmunds M. G., Smith G., 1980, MNRAS, 193, 219
Pagel B. E. J., Simonson E. A., Terlevich R. J., Edmunds M. G., 1992, MNRAS, 255, 325
Panagia N., 1973, AJ, 78, 929
Rubin R. H., Simpson J. P., Erickson E. F., Haas M. R., 1988, ApJ, 327, 377
Searle L., 1971, ApJ, 168, 327
Shaver P. A., McGee R. X., Newton L. M., Danks A. C., Pottasch S. R., 1983, MNRAS, 204, 53
Shortridge K., 1990, SERC Starlink User Note No. 86, Rutherford Appleton Laboratory
Simpson J. P., Colgan S. W., Rubin R. H., Erickson E. F., Haas M. R., 1995, ApJ, 444, 721
Stasińska G., 1980, A&A, 84, 320 (S80)
Stasińska G., 1982, A&AS, 48, 299 (S82)
Stone R. P. S., 1977, ApJ, 218, 767
Torres-Peimbert S., Peimbert M., Fierro J., 1989, ApJ, 345, 186
Tosi M., Díaz A. I., 1985, MNRAS, 217, 571
van der Hucht K. A., Conti P. S., Lundström I., Stenholm B., 1981, Space Sci. Rev., 28, 227
Vila-Costas B., Edmunds M. G., 1992, MNRAS, 259, 121
Vílchez J. M., 1989, ApSS, 157, 61
Vílchez J. M., Pagel B. E. J., 1988, MNRAS, 231, 257
Vílchez J. M., Pagel B. E. J., Díaz A. I., Terlevich E., Edmunds M. G., 1988a, MNRAS, 235, 633
Vílchez J. M., Edmunds M. G., Pagel B. E. J., 1988b, PASP, 100, 1428
Whitford A. E., 1958, AJ, 63, 201
Wouterloot J. G. A., Brand J., Burton W. B., Kwee K. E., 1990, A&A, 230, 21
Zaritsky D., Kennicutt R. C., Huchra J. P., 1994, ApJ, 420, 87